

Review

The promise of high-entropy materials for high-performance rechargeable Li-ion and Na-ion batteries

Wei Zheng,¹ Gemeng Liang,^{1,*} Qiong Liu,² Jingxi Li,¹ Jodie A. Yuwono,¹ Shilin Zhang,¹ Vanessa K. Peterson,³ and Zaiping Guo^{1,*}

SUMMARY

Our growing dependence on rechargeable Li/Na-ion batteries calls for substantial improvements in the electrochemical performance of battery materials, including cathodes, anodes, and electrolytes. However, the performance enhancements based on traditional modification methods of elemental doping and surface coating are still far from the target of high-performance rechargeable batteries. Fortunately, the recent emergence of high-entropy materials preserving a stable solid-state phase for energy-related applications provides unprecedented flexibility and variability in materials composition and electronic structure, opening new avenues to accelerate battery materials development. This perspective first presents clear qualitative and quantitative definitions for high-entropy battery materials, as well as summarizes the enhancement mechanisms. Then, we comprehensively review state-of-the-art research progress and highlight key factors in the rational design of advanced high-entropy battery materials from both experimental and calculational aspects. Moreover, the challenges limiting the progress of this research are presented, alongside insights and approaches to address these issues at the research forefront. Finally, we outline potential directions for extending the future development of the high-entropy strategy to solve other critical issues in battery materials research. This perspective will guide researchers in their studies toward the development of high-performance rechargeable Li-ion and Na-ion batteries.

INTRODUCTION

High-entropy (HE) materials usually consist of a single phase containing a large elemental diversity in the structure, in which interaction between multiple elements plays an important role in improving material performance, enabling the tailoring of properties to address performance limitations in functional materials during practical application.¹ To date, HE material families include alloys, oxides, carbides, borides, nitrides, etc., and are experiencing continuous growth in popularity.^{2,3} Among them, the playgrounds of HE ceramics can extend to diversified application areas, such as environmental protection, thermoelectricity, water splitting, catalysis, and energy storage devices, and lead to momentous technology revolutions.^{3,4} Due to their flexibility and variability in materials composition and electronic structure, respectively, HE ceramics promise to break through the performance bottlenecks of conventional battery materials in rechargeable Li/Na-ion batteries (LIBs/NIBs),

CONTEXT & SCALE

Developing high-performance battery materials such as cathodes, anodes, and electrolytes is regarded as one of the most important requirements to overcome the current performance limitations of rechargeable Li/Na-ion batteries. The targeted design of high-entropy materials has emerged as an alternative strategy to develop battery material performance, gaining rapidly in popularity. In this perspective, we outline the definition and mechanism for high-entropy battery materials, summarize state-of-the-art research on the development of high-entropy battery materials, and discuss progress limitations, highlighting design principles and development directions. Overall, this perspective may stimulate and reinforce future rechargeable Li/Na-ion battery research.

opening new avenues in the design of high-performance electrochemical energy storage devices.^{5,6}

Compared with conventional doping that primarily involves one or two elements, HE approaches deliver more flexibility in structural design, offering a larger diversity of crystal and electronic structure. Moreover, short-range interruptions of the crystal structure as a result of elemental diversity both increase tolerance to structural evolution during electrochemical processes and simultaneously induce defects beneficial to electron and ion migration. The implementation of HE design approaches in rechargeable LIBs/NIBs materials began in 2016 with the rock-salt-type structures, $(\text{Mg}, \text{Co}, \text{Ni}, \text{Cu}, \text{and Zn})_{1-x}\text{Li}(\text{Na})_x\text{O}$ as solid-state electrolyte,⁷ continued in 2018 with the $(\text{Co}_{0.2}\text{Cu}_{0.2}\text{Mg}_{0.2}\text{Ni}_{0.2}\text{Zn}_{0.2})\text{O}$ anode,⁸ and in 2019 with the $\text{Li}_x(\text{Co}_{0.2}\text{Cu}_{0.2}\text{Mg}_{0.2}\text{Ni}_{0.2}\text{Zn}_{0.2})\text{O}_x$ cathode,⁹ igniting further development of high-performance rechargeable LIBs/NIBs. The success of HE rock-salt materials stimulates the successful exploration of other different structural types of battery materials, such as transition metal (TM)-layered-type-structured materials,¹⁰ sodium superionic conductor/lithium superionic conductors (NASICON/LISICONs),¹¹ spinel-type-structured materials,¹² perovskite-type-structured materials,¹³ Prussian blue analogs,¹⁴ and garnet-type-structured materials,^{15,16} which presents unprecedented improvements in both mechanistic behaviors and electrochemical properties. For example, the Ni-rich-layered cathode $\text{LiNi}_{0.8}\text{Mn}_{0.13}\text{Ti}_{0.02}\text{Mg}_{0.02}\text{Nb}_{0.01}\text{Mo}_{0.02}\text{O}_2$ possesses an unprecedented zero volumetric change during Li^+ intercalation and deintercalation, favorable for long battery life and leading to 98.5% capacity retention after 100 cycles in the voltage range 2.5–4.4 V, which stands out from other Ni-rich candidates with traditional doping modification.¹⁷ The micrometer-sized $\text{Mg}_{0.2}\text{Co}_{0.2}\text{Ni}_{0.2}\text{Cu}_{0.2}\text{Zn}_{0.2}\text{O}$ anode delivers an extraordinarily high battery capacity alongside superior cycling stability, performing 500 cycles without any significant capacity degradation, which overcomes the “size effect” in the conversion reaction of metal oxides.⁸ HE-induced short-range structural distortion in NASICON/LISICON/garnet-type solid-state electrolytes results in an overlapping distribution of surrounding alkali-ion site energy, creating a percolation network that enables enhanced ionic conductivity.¹⁶

Although HE strategy opens various possibilities for optimizing different battery materials, state-of-the-art research regarding HE battery materials (HEBMs) is still in its infancy, and many fundamental concepts for HEBMs are vague, resulting in some ambiguities and controversies, such as the definition of HE materials, HE mechanism in HEBMs, the difference between HE materials and entropy-stabilized materials, etc., which may hamper the development of HEBMs. Besides that, further investigations are paramount to clarifying the underlying working mechanism of multicomponent effects on material property and providing a clear insight into the future direction for developing HEBMs. It is therefore urgently necessary to study the relationship between the multi-component structure and electrochemical performance of HEBMs, as well as to build clear design rules. In this perspective, we provide the definition of HE materials based on quantitative and quantitative aspects and highlight the HE mechanism according to the features of battery materials. We outline state-of-the-art research into HEBMs as cathodes, anodes, and electrolytes for rechargeable LIBs/NIBs and discuss the effects of the multi-component structure in improving structural stability during electrochemical processes. We address the design principles of HEBMs, point out issues in current research approaches, and provide insights into possible solutions. Finally, we highlight future directions for the development of HEBMs toward exceptional electrochemical performance.

¹School of Chemical Engineering, The University of Adelaide, Adelaide, SA, Australia

²Department of Materials Engineering, KU Leuven, Kasteelpark Arenberg, Leuven, Belgium

³Australian Centre for Neutron Scattering, Australian Nuclear Science and Technology Organisation, Sydney, NSW, Australia

*Correspondence:
gemeng.liang@adelaide.edu.au (G.L.),
zaiping.guo@adelaide.edu.au (Z.G.)

<https://doi.org/10.1016/j.joule.2023.10.016>

DEFINITION AND HE MECHANISM OF HE MATERIALS

The concept of HE in materials dates back to 2004 when pioneering work by Yeh et al.¹⁸ first considered this concept for alloys, where structural mismatch and limited ion solubility issues could be addressed by increasing configurational entropy. There are two different ways (qualitative or quantitative) to describe HE materials:

Qualitatively, Yeh et al.¹⁸ first described HE alloys based on the composition features. HE alloys contain a minimum of five primary elements, each with an atomic concentration between 5% and 35%, therefore extending the HE concept to broader compositional ranges for materials such as layered-type-structured oxide cathodes¹⁷ NASICON-structured cathodes.¹¹ In these reports,^{11,17} the incorporation of approximately five elements or more at the same crystal site was considered HE. More recently, this concept was considered for liquid, where the combination of multiple salts or solvents in a liquid electrolyte was referred to as HE.^{19,20} Although straightforward and useful, such qualitative descriptions of HE materials lack clear boundaries, making it difficult to distinguish high from medium-/low-entropy materials.

Quantitatively, the value of configurational entropy (S_{config}) could be used to classify the HE materials. In alloy, the degree of configurational entropy (S_{config}) can be evaluated as Equation 1²¹:

$$S_{\text{config}} = -R \left(\sum_{i=1}^N x_i \ln x_i \right) \quad (\text{Equation 1})$$

in which N is the number of elemental species, x_i is the mole fraction of component i , and R is the universal gas constant ($R = 8.314 \text{ J K}^{-1} \text{ mol}^{-1}$). Materials with $S_{\text{config}} \geq 1.5 R$ are considered HE, whereas those with $1.5 R > S_{\text{config}} \geq 1 R$ and $S_{\text{config}} < 1 R$ are considered to be medium- and low-entropy systems, respectively. In 2015, the concept of HE was introduced to rock-salt oxides, with these materials containing both cations and anions, and the configurational entropy for these materials is evaluated as Equation 2⁸:

$$S_{\text{config}} = -R \left[\left(\sum_{i=1}^M x_i \ln x_i \right)_{\text{cation-site}} + \left(\sum_{i=1}^N x_j \ln x_j \right)_{\text{anion-site}} \right] \quad (\text{Equation 2})$$

in which M and N are the number of cationic and anionic elemental species, respectively, x_i and x_j are the mole fraction of ions at cation and anion sites, respectively. The configurational entropy calculation was then extended further to oxides presenting multiple-cationic sites, such as perovskite oxides with formula ABO_3 (A and B represent cations in 12 and 6 coordinated sites, respectively. O represents oxygen element.), evaluated as Equation 3²²:

$$S_{\text{config}} = -R \left[\left(\sum_{i=1}^M x_a \ln x_a \right)_{\text{A cation-site}} + \left(\sum_{i=1}^L x_b \ln x_b \right)_{\text{B cation-site}} + \left(\sum_{i=1}^N x_j \ln x_j \right)_{\text{anion-site}} \right] \quad (\text{Equation 3})$$

where x_a , x_b , and x_j are the mole fraction of elements at the A-site, B-site, and anion site, respectively, and where M , L , and N are the number of cations at the A-site, B-site, and anion site, respectively. These quantitative definitions enable an explicit boundary to be created by which HE materials can be classified. However, this definition limits the application of the HE concept to emerging areas, such as for liquid electrolytes as mentioned above. Furthermore, it is difficult to accurately calculate the exact value of configuration entropy of some materials such as battery materials.

For example, many battery materials possess some defects, such as oxygen vacancies and anti-site defects, which can impact the configuration entropy.

Similar to HE alloys,²³ HE mechanisms for HEBMs could be summarized to four core effects based on the features of battery materials, i.e., HE effect, diffusion retard effect, lattice distortion effect, and cocktail effect:

HE effect: The elevated configurational entropy in materials could reduce the free energy of solid solution phases and thereby contribute to their formation, according to the Gibbs-Helmholtz equation²⁴:

$$\Delta G_{mix} = \Delta H_{mix} - T\Delta S_{mix} \quad (\text{Equation 4})$$

in which ΔG_{mix} , ΔH_{mix} , and ΔS_{mix} are the free energy, enthalpy, and entropy, respectively, and T is the reaction temperature. HE strategy could improve the configuration entropy in a system, thereby increasing the value of ΔS_{mix} . This provides a possibility to overcome the energy barrier of enthalpy to form a solid-state phase at higher temperatures in battery materials. It should be noted that other factors, such as defects, could influence the solid-state phase stability. Furthermore, experimental confirmation of the configurational entropy as the dominant factor in the formation of a solid-state phase may justify the categorization of a material as entropy stabilized.²⁵ Right to now, in HEBMs, only rock-salt type ($\text{Co}_{0.2}\text{Cu}_{0.2}\text{Mg}_{0.2}\text{Ni}_{0.2}\text{Zn}_{0.2}\text{O}$) compound has been proved to be classified as an entropy-stabilized material.¹

Diffusion retard effect: The diffusion of multiple ions and the associated phase transformations within HEBMs exhibit a slower rate in comparison to conventional materials. In HEBMs, multiple ions are usually incorporated into TM sites and not involved in the de/intercalation process.²⁶ Differences in the neighboring atoms between crystal sites may increase the migration barrier for jump diffusion between those sites, reducing the unwanted migration of metals. The suppression of such migration may also hinder phase transformation processes, as such process requires the coordinated diffusion of many elements and uniform gliding of TM layer, which is witnessed in many HE-layered cathodes.^{10,17}

Lattice distortion effect: Structures with elements of a variety of ionic sizes may lead to the distortion of the structural lattice, affecting the behavior of charge-carrying ions in battery materials such as Li^+ and Na^+ , thus impacting material properties. For example, short-range structure distortions in a HE solid electrolyte have led to overlapping site energies for alkali ions, facilitating their percolation during electrochemical function.¹⁶ Similarly, a highly distorted structure lattice of a metal oxide anode produced defects, promoting electron and Li^+ and Na^+ migration.⁵

Cocktail effect: In HEBMs, electrochemical performance has been shown to not only depend on the average property of individual-doped element components but also on effects from inter-elemental interaction. Therefore, the HE feature can lead to positive and different effects within HEBMs to enhance their electrochemical performance. For example, micron-sized metal oxide anodes suffer from poor ionic conductivity and severe structural instability, with these issues known as size effects. Due to the cocktail effects of multi-cations synergy, the pristine structure would transform into multiple metallic and oxide nanostructures after the first discharge process and turn into a composite with intrinsic semi-coherent metal/oxide nanophase after cycles. The self-assembled nanostructures grown in the micron-sized

particles enable fast electron and ion diffusion and preserve high structure stability, thus improving the electrochemical performance.²⁷

HEBMs

HEBMs, where multiple elements are distributed among metal sites, are synthesized through mainly conventional methods such as solid-state sintering, sol-gel, and co-precipitation techniques, where the temperature and hold time are key parameters influencing the formation of a single-phase material.⁴ Structural characterization of HEBMs is typically performed using methods such as X-ray diffraction (XRD) and neutron powder diffraction (NPD) to identify phase composition as well as scanning electron microscopy (SEM) with energy dispersive X-ray spectroscopy (EDS) and scanning transmission electron microscopy (STEM) to identify the elemental distribution. The electronic structure and short-range geometry of the metals in HEBMs are usually investigated using tools such as X-ray absorption spectroscopy (XAS). The electrochemical performance of these materials is evaluated using standard approaches, and material characterization techniques are applied *ex situ/in situ* to understand the material structural and charge evolution during electrochemical activity.

HE cathodes

The cathode remains the performance limitation of current rechargeable LIBs/NIBs. During the extremities of Li^+/Na^+ de/intercalation, the cathode usually experiences an irreversible phase transition and corresponding migration of TMs within the structure, leading to severe structural degradation and rapid capacity decay upon cycling. To date, the HE strategy has been successfully applied in different types of cathodes to improve performance, including layered TM oxides, disordered rock-salt oxides, and NASICON and Prussian blue analog cathodes.

Layered structure cathodes

TM oxides with a layered-type structure are composed of sheets of edge-shared TMO_6 octahedra (the TM layer), with alkali ions located between neighboring TMO_6 sheets (the alkali layer). Delmas et al.²⁶ categorized these layered compounds based on the number of TM layers in a stacking unit and the coordination environment of alkali ions (O or P represents an octahedral or prismatic coordination environment). O3-type Ni-rich-layered oxides for LIBs are considered the most promising cathodes for automotive applications due to their high energy density and relatively low cost.²⁸ However, they suffer from large volume changes of the bulk structure and loss of oxygen at the surface, where the formation of the H3 phase results in anisotropic shrinkage of the crystal structure and strong oxidizing substances promote side reaction, leading to rapid battery failure.^{29,30} Furthermore, inherently poor thermal stability of the de-lithiated Ni-rich material hampers practical application.³¹ Zhang et al.¹⁷ reported the Ni-rich and Co-free HE cathode $\text{LiNi}_{0.8}\text{Mn}_{0.13}\text{Ti}_{0.02}\text{Mg}_{0.02}\text{Nb}_{0.01}\text{Mo}_{0.02}\text{O}_2$ (HE-LNMO). The detailed structural parameters can be found in Table S1. The HE-LNMO exhibits an even higher performance than the well-known commercial $\text{LiNi}_{0.8}\text{Mn}_{0.1}\text{Co}_{0.1}\text{O}_2$ (NMC-811) material, including higher initial Coulombic efficiency (94%), excellent cycling performance (98.5% capacity retention after 100 cycles within 2.5–4.4 V), and good cycle retention at 50°C (96.6% after 50 cycles), whereas these for NMC-811 are just 82%, 87.1%, and 90.3%, respectively. Synchrotron-based X-ray powder diffraction showed that HE-LNMO exhibits a maximum volume change of 0.3% over 2.7–4.3 V in the first cycle and thereby could be qualified as promising “zero strain” materials. Besides that, as shown in Figure 1A, synchrotron-based transmission X-ray microscopy (TXM) and SEM data confirm that no obvious cracks are observed in the HE-LNMO after long

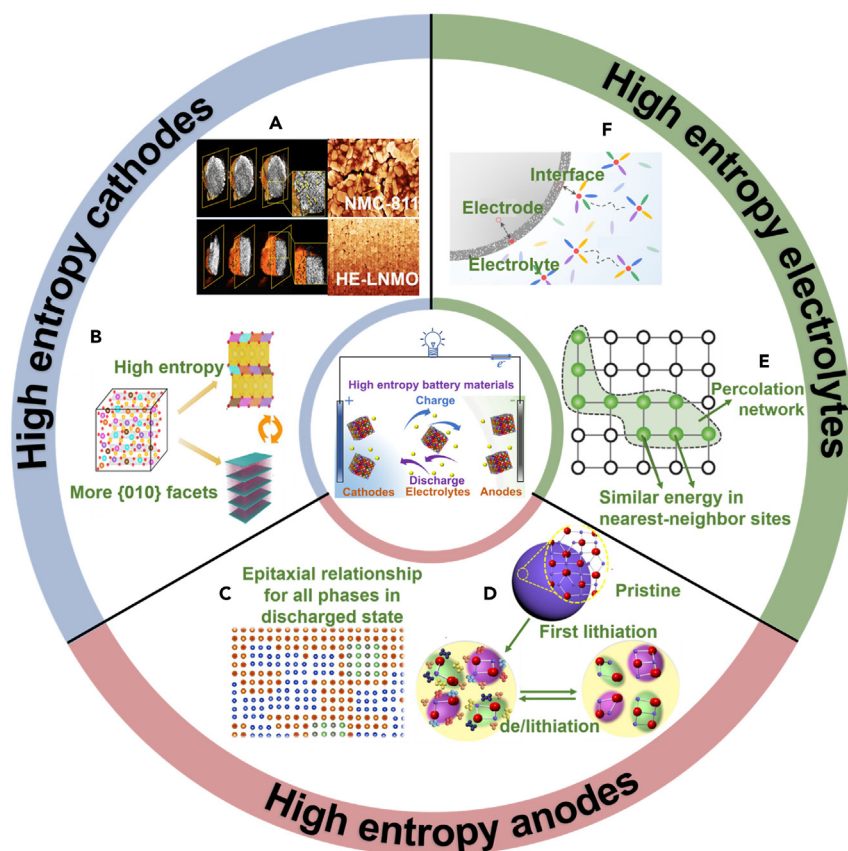


Figure 1. Typical HEBMs for rechargeable LIBs/NIBs

(A) Substantial cracking during cycling identified in NMC-811 by synchrotron-based TXM and SEM, compared with relatively few cracks in HE-LNMO (adapted from Zhang et al.¹⁷ with permission. Copyright 2022, Nature Publishing Group).

(B) High-performance P2-type cathode with a high percentage of {010} facets as facilitated by high entropy (adapted from Fu et al.³² with permission. Copyright 2022, The Authors).

(C) Epitaxial semi-coherent metal/oxide nanophase composite created after the first discharge in a high-entropy rock-salt type anode material (adapted from Wang et al.²⁷ with permission. Copyright 2023, The Authors).

(D) Atomic-scale microstructure evolution during de/lithiation processes in metal oxide anode (adapted from Huang et al.³³ with permission. Copyright 2021, Elsevier B.V.).

(E) Schematic of the percolation network in high-entropy solid electrolyte materials, in which the nearest-neighbor sites share similar energies (adapted from Zeng et al.¹⁶ with permission. Copyright 2022, The Authors).

(F) Schematic of the high-entropy liquid electrolyte system (adapted from Wang et al.¹⁹ with permission. Copyright 2023, The Authors).

cycles. The superior structural stability of HE-LNMO can be attributed to the multi-elemental composition that creates HE configurations, suppressing the loss of oxygen, cation mixing, and detrimental phase transformation at the extremities of lithium concentration.

O3-type Li-rich Mn-based-layered cathodes with both cationic and anionic redox activity exhibit extraordinarily high specific capacities (above 250 mAh g^{-1}).³⁴ However, anionic redox activity is usually accompanied by irreversible TM intra-/inter-layer migration and oxygen loss, leading to severe capacity degradation and voltage decay.³⁵ $\text{Li}_{1.0}[\text{Li}_{0.15}\text{Mn}_{0.50}\text{Ni}_{0.15}\text{Co}_{0.10}\text{Fe}_{0.025}\text{Cu}_{0.025}\text{Al}_{0.025}\text{Mg}_{0.025}]\text{O}_2$ (E-LRM) HE material is developed by Song et al.³⁶ (detailed structural parameters could be

found in Table S1), exhibiting a high specific capacity of 260 mAh g^{-1} and an excellent cycle stability of 93% after 100 cycles at 25 mA g^{-1} , in which Co^{3+} , Ni^{2+} , Fe^{3+} , and Cu^{2+} act as redox centers in the electrochemical process, Li^+ , Mg^{2+} , and Al^{3+} form the Li-O-Li, Li-O-Mg, and Li-O-Al configurations that drive anionic redox activity, providing additional capacity and stabilizing the oxygen in the structure, with Mn^{4+} serving to further stabilize the structure. Studies show that the diversity of TMO_6 octahedra in the interlayer in E-LRM increases the energy for cooperative distortion of Mn^{4+} , mitigating against low-potential redox activity and short-range structure evolution.³⁶

O3-type Na-layered oxides for application as cathodes in NIBs have gained research attention due to their high theoretical capacity, facile manufacture, and low cost.³⁷ Nevertheless, these materials experience complex phase transitions during charge/discharge processes.³⁸ Zhao et al.¹⁰ reported the HE O3-type-layered cathode material $\text{NaCu}_{0.12}\text{Ni}_{0.12}\text{Mg}_{0.12}\text{Co}_{0.15}\text{Fe}_{0.15}\text{Mn}_{0.1}\text{Ti}_{0.1}\text{Sn}_{0.1}\text{Sb}_{0.04}\text{O}_2$ (HEO-O3), with a high capacity retention of 83% after 500 cycles and Coulombic efficiencies as high as 99% (detailed structural parameters can be found in Table S1). Reversible phase transformation between O3 and P3 type structures was observed using *in situ* XRD, accompanied by interesting hysteresis in the phase evolution, resulting in 60% of the total capacity being stored in the O3 type structure. It was shown that the multi-elemental doping in HEO-O3 led to a more random distribution of redox centers in the TM layer, guarding against detrimental effects of structural changes during electrochemical processes.

Compared with O3-type structures, P2-type-layered structures preserve highly accessible Na-ion diffusion pathways and have only moderate phase evolution during function, attracting increasing worldwide attention.³⁹ HE strategy in P2-type cathodes could contribute to partially mitigate phase evolution to intermediate OP4 phase or entirely suppress the phase evolution to preserve P2 phase during electrochemical process in the structure, thereby significantly improving rate performance. Yang et al.⁴⁰ prepared the HE P2-type material $\text{Na}_{0.6}(\text{Ti}_{0.2}\text{Mn}_{0.2}\text{Co}_{0.2}\text{Ni}_{0.2}\text{Ru}_{0.2})\text{O}_2$ with high-rate performance (detailed structural parameters can be found in Table S1). This material delivers a discharge capacity of 164 mAh g^{-1} at 20 mA g^{-1} and a high capacity of 68 mAh g^{-1} at $17,200 \text{ mA g}^{-1}$. During electrochemical processes, this material presents a reversible phase evolution from P2 to OP4 phase. The exceptional rate performance of this HE material is verified both experimentally and theoretically to originate from the mitigation of Na^+ /vacancy ordering and phase evolution, as well as the creation of a percolating diffusion network for Na^+ .⁴⁰ As shown in Figure 1B, Fu et al.³² found that HE P2 type materials $\text{Na}_{0.62}\text{Mn}_{0.67}\text{Ni}_{0.23}\text{Cu}_{0.05}\text{Mg}_{0.09-2y}\text{Ti}_y\text{O}_2$ (detailed structural parameters could be found in Table S1) with increased entropy and high percentage of {010} facets could effectively stabilize the crystal structure in P2 phase and optimize electrochemical kinetics of anionic redox reaction, thus contributing to fast Na^+ diffusion. For example, $\text{Na}_{0.62}\text{Mn}_{0.67}\text{Ni}_{0.23}\text{Cu}_{0.05}\text{Mg}_{0.07}\text{Ti}_{0.01}\text{O}_2$ has an outstanding capacity of 82.6 mAh g^{-1} at $1,200 \text{ mA g}^{-1}$, in contrast with that of $\text{Na}_{0.62}\text{Mn}_{0.67}\text{Ni}_{0.37}\text{O}_2$ (40 mAh g^{-1}).

Rock-salt structure cathodes

Disordered rock-salt-type-structured cathodes for LIBs are comprised of a close-packed oxygen framework with a nominally random distribution of Li and TM at cationic octahedral interstitial sites. With high Li excess, these cathodes achieve extremely high specific capacity ($>300 \text{ mAh g}^{-1}$) and high specific energy density ($\sim 1,000 \text{ Wh kg}^{-1}$) as a result of cationic and anionic redox activity.⁴¹ Nevertheless,

short-range cation ordering in the structure may influence the Li site environment and impact long-range Li transport, resulting in unsatisfactory rate performance.⁴² Lun et al.⁴³ compared a series of such cathodes with low, medium, and high entropies: $\text{Li}_{1.3}\text{Mn}^{3+}_{0.4}\text{Ti}_{0.3}\text{O}_{1.7}\text{F}_{0.3}$ (TM2), $\text{Li}_{1.3}\text{Mn}^{2+}_{0.2}\text{Mn}^{3+}_{0.2}\text{Ti}_{0.1}\text{Nb}_{0.2}\text{O}_{1.7}\text{F}_{0.3}$ (TM4), and $\text{Li}_{1.3}\text{Mn}^{2+}_{0.1}\text{Co}^{2+}_{0.1}\text{Mn}^{3+}_{0.1}\text{Cr}^{3+}_{0.1}\text{Ti}_{0.1}\text{Nb}_{0.2}\text{O}_{1.7}\text{F}_{0.3}$ (TM6), respectively. TM6 has both high specific capacity and rate performance, delivering a reversible specific capacity of 307 mAh g^{-1} at 20 mA g^{-1} and more than 170 mAh g^{-1} at $2,000 \text{ mA g}^{-1}$ (detailed structural parameters can be found in Table S1). By comparison, TM2 produced only 220 and 58 mAh g^{-1} , respectively. HE strategy could prevent the formation of a single dominant short-range order in the structure to preserve accessible 0-TM percolation of Li transport, thus facilitating rate performance during electrochemical processes.

NASICON cathodes

The first NASICON material was reported in 1976 by Goodenough et al.,⁴⁴ which exhibits advantages in three-dimensional (3D) open framework, tunable redox potentials, and high thermodynamic stability as cathodes for NIBs. However, due to the multi-Na-ions de/intercalation process, they experience severe structural evolution, including large volume changes and phase transformation from monoclinic to rhombohedral at high voltage ($>3.8 \text{ V}$ vs. Na), leading to capacity degradation.⁴⁵ Li et al.⁴⁶ developed a HE $\text{Na}_{3.4}\text{Fe}_{0.4}\text{Mn}_{0.4}\text{V}_{0.4}\text{Cr}_{0.4}\text{Ti}_{0.4}(\text{PO}_4)_3$ (H-NVP) NASICON cathode with five different TM species (detailed structural parameters could be found in Table S1), with the material delivering a specific capacity of 161.3 at 15 mAh g^{-1} in the voltage range $1.5\text{--}4.5 \text{ V}$ and maintaining 85.3% of this capacity after 1,000 cycles. *In situ* XRD demonstrated that H-NVP presents a stable trigonal phase and undergoes only minor volume change during electrochemical reactions, enabling cycle stability.

Prussian blue analog cathodes

Prussian blue analogs are efficient sodium storage materials with an open channel structure and abundant redox-active sites. Nevertheless, a low-specific capacity and poor reversibility, caused by phase transition during charge/discharge processes, have limited the practical application of Prussian blue analogs as electrodes.⁴⁷ Ma et al.¹⁴ introduced five different TM species at the nitrogen site in the $\text{Na}_x(\text{FeMnNiCuCo})[\text{Fe}(\text{CN})_6]$ (HE-PBA) material, a HE vacancy-containing Prussian blue analog (detailed structural parameters can be found in Table S1). The HE-PBA electrode delivered a high specific capacity of 120 mAh g^{-1} at 10 mA g^{-1} between 2 and 4.2 V during the first cycle, maintaining 94% of this initial capacity after 150 cycles. *In situ* XRD with this cathode showed that HE-PBA is almost strain-free during this electrochemical activity, with the cubic lattice parameter varying only between 10.23 and 10.31 \AA . The enhancement of capacity and structural stability can be attributed to the presence of several active redox reactions.

HE anodes

Research into HE materials as anodes has mainly focused on metal oxides, regarded as appealing anode candidates due to their low cost and high gravimetric specific capacity. Nevertheless, the primary obstacle that restricts their practical utilization is the unsatisfactory cyclability owing to severe structural destruction.¹² Broadly, HE metal oxide anodes can be categorized into rock-salt, spinel, and perovskite-type structures.

Rock-salt structure anodes

As the first reported HE anode, rock-salt-type-structured $\text{Mg}_{0.2}\text{Co}_{0.2}\text{Ni}_{0.2}\text{Cu}_{0.2}\text{Zn}_{0.2}\text{O}$ with micrometer particle size gained great attention (detailed structural

parameters can be found in Table S1), which exhibits a specific capacity above 650 mAh g^{-1} at 0.2 A g^{-1} and maintains stable capacity retention over 500 cycles, thereby overcoming the size effect observed in conventional metal oxides during the conversion reaction.⁸ Wang et al.²⁷ addressed the enhancement mechanism in these materials through characterization of their charge states evolution and the microstructure at different electrochemical states. Their works found that although Zn and Co contribute to capacity, it is Mg that stabilizes the oxide phase, enabling the accommodation of Li^+ , Co^{2+} , and Zn^{2+} at the charged state, whereas Cu and Ni maintain the structural integrity of the nanoscale 3D metallic network after the first discharge cycle. On cycling, the micron-sized particles transform into an epitaxial semi-coherent metal/oxide nanophase material composite, featuring superior structural stability (Figure 1C).

Spinel-structure anodes

Compared with rock-salt-type structures, the spinel structure could provide more effective Li^+ transport paths to enhance the electrochemical performance. The HE spinel oxide $(\text{CrNiMnFeCu})_3\text{O}_4$ anode delivered an unprecedented high specific capacity of 800 and 480 mAh g^{-1} at 50 and $2,000 \text{ mA g}^{-1}$, respectively (detailed structural parameters could be found in Table S1), with extraordinary capacity retention of 100% after 400 cycles.⁴⁸ Huang et al.³³ investigated the conversion behavior in $(\text{CrNiMnFeCu})_3\text{O}_4$ during charge-discharge cycles at the atomic scales. As shown in Figure 1D, they found that after the first lithiation to 0.5 V , $(\text{CrNiMnFeCu})_3\text{O}_4$ phase segregates into two new spinel phases, namely $\text{Cr}_x\text{Fe}_{3-x}\text{O}_4$ and $\text{LiNi}_x\text{Co}_{1-x}\text{O}_2$, which acts as a structural stabilizer and is responsible for the great electrode cycling performance. Further lithiation to 0.01 V leads to the precipitation of metallic Fe, Cr, Ni, and Co nanocrystals from the part of spinel-structure frameworks. The remaining spinel phases act as seeds that grow by devouring surrounding metal nanoparticles during delithiation.

Perovskite structure anodes

Perovskite (ABO_3)-type structure material preserves easily cation substitution sites and rich oxygen vacancy, considered a promising anode. Jia et al.¹³ prepared a series of HE porous perovskite-type anodes $\text{RE}(\text{Co}_{0.2}\text{Cr}_{0.2}\text{Fe}_{0.2}\text{Mn}_{0.2}\text{Ni}_{0.2})\text{O}_3$ ($\text{RE} = \text{La}$, Sm , and Gd), with the material $\text{Gd}(\text{Co}_{0.2}\text{Cr}_{0.2}\text{Fe}_{0.2}\text{Mn}_{0.2}\text{Ni}_{0.2})\text{O}_3$ exhibiting a large discharge capacity of 403 mAh g^{-1} at 0.2 A g^{-1} and an excellent rate capacity of 207 mAh g^{-1} at 2.0 A g^{-1} (detailed structural parameters can be found in Table S1). The lattice distortion based on HE strategy in this material contributes to the enriched oxygen vacancies and mesoporous structure, which enhances the rate capacity and cycling stability during electrochemical processes.¹³

HE electrolytes

Solid-state electrolytes

Solid-state electrolytes, as a promising electrolyte in the development of high-performance LIBs/NIBs, deliver advantages of higher safety, stability, and energy density than traditional liquid electrolyte.⁴⁹ However, commercial application of all solid-state batteries is hindered by their poor ionic conductivity and interfacial instability. Jung et al.⁵⁰ report a HE garnet-type solid-state electrolyte $\text{Li}_7\text{La}_3\text{Zr}_{0.4}\text{Hf}_{0.4}\text{Sn}_{0.4}\text{Sc}_{0.4}\text{Ta}_{0.4}\text{O}_{12}$ (detailed structural parameters can be found in Table S1), with high Li content that possesses a lower formation temperature of 400°C (cf. 750°C) and better reduction stability against lithium metal when compared with the equivalents with low Li content. Zeng et al.¹⁶ demonstrated the use of HE strategy to improve ionic conductivity by orders of magnitude in NASICON/LISICON/garnet-type-structured solid-state electrolytes. In well-ordered structures, such as

$\text{Li}_3\text{Nd}_3\text{Te}_2\text{O}_{12}$, the energy difference between the $\text{Li}_{24\text{d}}$ and $\text{Li}_{48\text{g}}$ sites is 1.57 eV, which is the minimum energy barrier for percolating ion hopping. However, when the local bond distortion is introduced, the calculated value is reduced to 0.39 eV. Such tendency is further confirmed in $\text{Li}_{1+x}\text{Al}_x\text{Ti}_{2-x}(\text{PO}_4)_3$ and $\text{Na}_{3+x}\text{Zr}_2(\text{SiO}_4)_{2+x}(\text{PO}_4)_{1-x}$. HE materials, such as $\text{Li}_3(\text{LaPrNd})_3(\text{TeW})_2\text{O}_{12}$, $\text{NaTi}_{1/2}\text{Zr}_{1/2}\text{Sn}_{1/2}\text{Hf}_{1/2}\text{P}_3\text{O}_{12}$, and $\text{LiTi}_{1/2}\text{Zr}_{1/2}\text{Sn}_{1/2}\text{Hf}_{1/2}\text{P}_3\text{O}_{12}$ (detailed structural parameters could be found in Table S1), present an improved ionic conductivity when compared that with traditional ones. Short-range structure distortion enabled by HE strategy in these materials significantly reduced the activation energy for alkali-ion diffusion through the generation of a network of interconnected sites, enhancing ionic conductivity (Figure 1E).

Liquid electrolytes

The integration of the HE strategy into liquid electrolytes can be achieved by introducing multiple salts. Wang et al.¹⁹ prepared a HE liquid electrolyte by combining 0.15 M lithium bis(fluorosulfonyl) imide, 0.15 M lithium bis(trifluoromethanesulfonyl)imide, 0.15 M lithium difluoro(oxalato)borate, and 0.15 M lithium nitrate in the single dimethoxyethane solvent. The combination of multiple anions in the electrolyte led to a diversity in solvation structures, decreasing the solvation strength between lithium ions and the solvents/anions, and promoting lithium ions diffusion and the formation of stable interphase passivation layers (Figure 1F).

PERSPECTIVES

The HE strategy has emerged as a new paradigm to accelerate the development of novel battery materials with promising properties and is receiving growing worldwide attention, together with significant research work launched as summarized above. However, debates on the functional mechanism persist in the literature, and our understanding of state-of-the-art HEBMs is still in its infancy. Although further studies are underway to explore the relationship between structure and property in HEBMs, issues and challenges remain to be addressed.

HEBM design

The compositional complexity of HEBMs is both the foundation for their cocktail of beneficial effects in improving electrochemical performance and the difficulty in materials design. There are two main aspects of HEBM design: element selection and component stoichiometry. HEBMs have strict requirements for elemental selection, arising from structural and functional criteria. Structural criteria involve considerations of ionic radius, valence state, and chemical and redox compatibility. Specifically speaking, multi-elemental inclusion at the same crystallographic site necessitates a similar ionic radius and the preservation of electrical neutrality. Furthermore, charge transfer between co-existing elements should be avoided, such as between Mn^{3+} and V^{3+} at the same crystallographic site, forming reduced Mn^{2+} and oxidized V^{5+} . Thus, cation pairs that are not redox-compatible should be excluded from the selection process. As for the functional criteria, different elemental groups are expected to offer distinct effects during electrochemical processes. Electrochemically active ions such as Ni^{2+} , Co^{3+} , Mn^{2+} , Cu^{2+} , Fe^{2+} , and Cr^{3+} should be included as redox centers to contribute to battery capacity, and electrochemically inactive ions such as Mn^{4+} , Sn^{4+} , Sb^{5+} , and Zr^{4+} are included to stabilize the host structure during the Li^+/Na^+ de/intercalation process. The inclusion of ions such as Li^+ , Na^+ , Mg^{2+} , and Zn^{2+} in TM cathodes can trigger anionic redox reactions to provide additional capacity.^{51,52} Besides that, some elements equipped with smaller/larger radius to the host structure may be considered to offer driving force for local lattice distortion, helping to enhance electrochemical stability.¹⁰ In considering component stoichiometry, there

is a trade-off between HE and high capacity, where incorporating additional cationic species may dilute the concentration of redox-active species, leading to lower specific capacity. Moreover, some species, such as Ti^{4+} and Zn^{2+} , when included in relatively high proportion, are less compatible with other ions and may lead to the occurrence of a secondary phase. Therefore, a thorough balance between these aspects should be taken into account in HEBM design.

Currently, HEBM research is mainly result-based driven through trial-and-error methods, which are both costly and slow, and it is therefore imperative to introduce theoretical calculations to predict the relationship between structure, composition, and electrochemical property. Hybrid Monte Carlo (MC), density functional theory (DFT), and molecular dynamics (MDs) approaches may assist in stoichiometry, structure, and atomic configurational (both short- and long-range) optimization of HEBMs.^{53–55} The rise of machine learning (ML) methods, such as neural networks or random forest approaches, may also assist this research by predicting structure and performance at the larger scale.^{56,57} As shown in Figure 2, combining MC, DFT, MD, and ML with experiments in an active learning loop may facilitate the identification of HEBMs with structures and compositions with favorable battery performance. First, a large range of parameters including composition and elemental species, phase and short/long-range structure, synthesis technique, and desirable property and performance could be harvested from a HEBMs database (Figure 2A). Then, for composition/phase selection, generative ML modeling using Wasserstein auto-encoder (WAE) and variational auto-encoder (VAE) algorithms (Figure 2B) could be used to generate initial composition and phase choices for battery materials by learning from massive data.⁵⁶ Calculation methods employing DFT, such as the pre-selected small set of ordered structures (PSSOS), may be used to further predict the short-range ordering of cations⁵³ (Figure 2C). After that, for theoretical validation, hybrid MC-MD simulation methods could be applied to assess the formation and stabilization feasibility of HE phases at specific temperatures.⁵⁴ (Figure 2D) The relationship between these HE structures and their properties can be investigated by ML using a two-stage ensemble regression method with multiple learning algorithms to predict electrochemical performance⁵⁷ (Figure 2E). High-throughput DFT is an essential tool to explore and predict battery material's behavior, notably around surface interactions including side reactions and surface structural evolution during electrochemical processes⁵⁵ (Figure 2F). The output of such theoretical work could be fed into experiments for verification. Material structure, morphology, electrochemical performance, and the mechanism for performance, such as charge compensation and phase evolution, could then be experimentally measured (Figure 2G). Finally, a selection of the most promising HEBMs would be ranked, and this information fed back into the HEBMs database (Figure 2H).

Understanding the improvement mechanism of HEBMs and extension of applicability

To date, the working mechanism of HEBMs is results-based and poorly understood, leading to some debates and contradictions regarding the functional mechanism for performance enhancement. For example, both fast and delayed O3-P3 phase transition behaviors found in the O3-type oxide electrodes ($\text{Na}_{2/3}\text{Li}_{1/6}\text{Fe}_{1/6}\text{Co}_{1/6}\text{Ni}_{1/6}\text{Mn}_{1/3}\text{O}_2$ ⁵⁸ and $\text{NaCu}_{0.12}\text{Ni}_{0.12}\text{Mg}_{0.12}\text{Co}_{0.15}\text{Fe}_{0.15}\text{Mn}_{0.1}\text{Ti}_{0.1}\text{Sn}_{0.1}\text{Sb}_{0.04}\text{O}_2$,¹⁰ respectively) are attributed to improving structural stability. Such discrepancies complicate an understanding of the mechanism of HE effects. Therefore, more comprehensive structural characterization encompassing a broader length scale, including those probing short-range order such as pair distribution function (PDF)

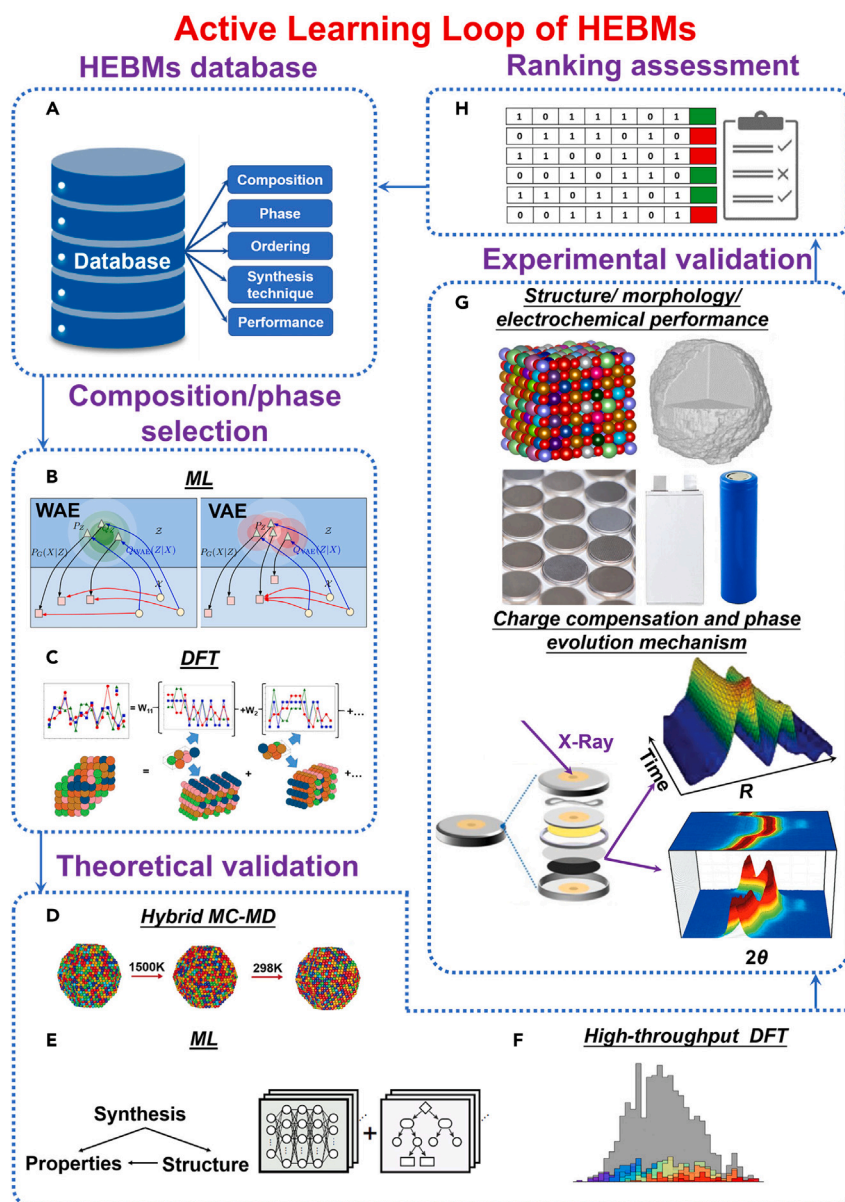


Figure 2. An active learning loop for the targeted compositional design and discovery of HEBMs

(A) HEBMs database.

(B) ML using WAE or VAE algorithms to generate initial composition and phase choices (adapted from Tolstikhin et al.⁵⁶ with permission. Copyright 2018, The Authors).

(C) The prediction of short-range ordering in HEBMs using the PSSOS method based on DFT (adapted from Sorkin et al.⁵³ with permission. Copyright 2022, The Authors).

(D) Hybrid MC-MD simulation approach to predict the possibility for the formation and stabilization of high-entropy phases at specific temperature (adapted from Yao et al.⁵⁴ with permission. Copyright 2020, The Authors).

(E) ML using two ensemble models composed of multilayer perceptions and gradient-boosting decision trees for further predicting electrochemical performance and structural stability (adapted from Rao et al.⁵⁷ with permission. Copyright 2022, The Authors).

(F) High-throughput DFT calculations for surface interaction behaviors among HEBMs (adapted from Battchelor et al.⁵⁵ with permission. Copyright 2020, The Authors).

(G) Experimental verification.

(H) Ranking assessment.

methods and XAS, is required to understand the structural distortion in HEBMs. Besides that, the mechanism of enhancement of electrochemical performance is normally attributable to the synergistic effects of multi-elemental inclusion in most HEBM studies. However, the detailed mechanism and distinct effects of the included elements on this enhancement remain unclear. Furthermore, introducing multi-elements could lead to significant lattice distortion in the crystal structure. Nevertheless, an explicit investigation for distortion level from the aspects of atoms, lattices, stacking faults, strain, etc. and their relationship with electrochemical performance are extremely scarce. Thus, intensive efforts in the following studies should be made to identify the functional groups and understand the role of individual elements during cycles and their relationship with peculiar effects in compounds. For instance, a comparison of TM–O bond lengths and angles within each TMO_6 octahedron in high- and low-entropy TM oxides may yield insight into the underlying structural stabilization mechanism associated with HE-facilitated performance.

Currently, the HE strategy has mainly focused on the modification of battery materials through the introduction of multi-elemental doping in the bulk crystal structure, whereas surface evolution at the electrode/electrolyte interphase, such as TM dissolution and side reactions with the electrolyte, has also been proven detrimental to electrochemical performance.⁵⁹ Such problems are difficult to address by modifying the bulk, and theoretically, HE surface approaches with coherent interfacial surface matching may provide a solution for these issues. Such functional HE layers have been proven effective, such as in $\text{LiNi}_{0.8}\text{Co}_{0.1}\text{Mn}_{0.1}\text{O}_2$ with enhanced electrochemical performance as a result of inhibited side reactions between the cathode and electrolyte.⁶⁰ Nevertheless, the underlying science of HE surface modification requires development, and future works are needed to extend the HE approach for battery material development. Second, we note that reports of HEBM research predominantly involve compositional modification, neglecting influencing factors such as synthesis methods, particle morphology, and size, and further effort to optimize these parameters to obtain HEBMs with excellent electrochemical performance is needed. Finally, adjusting the configuration entropy to regulate the electrochemical properties of materials recently became a research hotspot. Except for HEBMs, medium-entropy battery materials have gained some attention. For instance, Chen et al.⁶¹ designed a medium-entropy garnet material $\text{Li}_6\text{La}_3\text{Zr}_{0.5}\text{Hf}_{0.5}\text{Ta}_{0.5}\text{Nb}_{0.5}\text{O}_{12}$ as a solid-state electrolyte, which delivers a higher ionic conductivity when compared with $\text{Li}_6\text{La}_3\text{Zr}_{1.5}\text{Ta}_{1.5}\text{O}_{12}$. They further elucidated that four ions sharing the Zr site could regulate the bottleneck size and Li–O bond length to improve the ionic conductivity.⁶¹ Based on this, more attention should be paid to building a clear relationship between configuration entropy and electrochemical performance to guide the investigation of new battery materials.

Extension of the HE design to solve critical issues in battery performance

At present, HEBMs have shown great promise in enhancing the electrochemical performance of LIBs and NIBs, leading to an additional expectation for the HE strategy to tackle other issues in battery materials. In many battery materials, strain accumulation may induce catastrophic structure collapse and particle cracking, leading to rapid capacity decay. This normally originates from the massive volume changes in bulk phase evolution and the presentation of inhomogeneous phase due to TM migration, as well as lattice distortion along a uniform direction during electrochemical processes.^{62–64} Incorporating multi-components in the crystal structure could significantly inhibit the phase expansion/contraction and TM

migration by pillar effects and thus retard the extension of cracks caused by high strain in the particles. Moreover, homogeneously distributed HE compositions, i.e., cations, would accommodate structural changes in the local range, which may break the consolidated orientation and prevent lattice distorting along one direction, leading to an effective relieving of lattice strains. Furthermore, although many materials such as Li-rich materials,^{65,66} Na-layered TM oxides,³⁵ LiCoO₂ operated above 4.5 V,^{67,68} and LiNi_{0.5}Mn_{0.5}O₄ to 5.0 V,^{69–71} have been pursued with the aim of increasing energy density in LIBs/NIBs, charging to high voltage in these materials leads to structural degradation, jeopardizing their electrochemical performance. In Li-rich/Na-layered TM cathodes, charging to 4.8/4.5 V activates anionic redox to supplement additional capacity, but this is associated with oxygen release at the surface and the formation of molecular O₂ in the bulk, resulting in severe capacity decay and voltage hysteresis.³⁵ In the HE equivalent, interaction between oxygen ions and cations could be adjusted effectively due to abundant heterogeneous elements in TM layer, thus forming a steady oxygen state during electrochemical process. Charging LiCoO₂ or LiNi_{0.5}Mn_{0.5}O₄ to high voltage enables high capacity but leads to harmful phase transitions, such as the occurrence of H1-3/O1 phase in LiCoO₂ and rock-salt phase in LiNi_{0.5}Mn_{0.5}O₄, which induces rapid capacity degradation.^{70,72} Previous reports show the success of binary or ternary doping in inhibiting detrimental phase evolution of battery materials at high voltage,^{34,67} and broadening the elemental composition of LiCoO₂ and LiNi_{0.5}Mn_{0.5}O₄ materials by HE strategy may enhance structural stability. Metal oxide anodes, which experience conversion-type electrochemical reactions during charge/discharge, usually exhibit a high-voltage plateau during discharge processes due to the features of energy band structure, limiting the battery output power. The electronic structures in HE metal oxide anodes could be effectively regulated by dispersing various cations to achieve a low redox voltage and resultant high energy density of rechargeable LIBs/NIBs.

In summary, the HE strategy has emerged as a promising approach for addressing the inherent limitations of battery materials. As shown in [Tables S2](#) and [S3](#), compared with traditional battery materials, in cathodes, due to the diffusion retard effect of HE strategy, the harmful phase evolution during electrochemical processes could be suppressed in the HE-layered/NASICON/Prussian blue type cathodes, thus improving the electrochemical performance. In metal oxide anodes, the cocktail effect of multi-elemental components could be attributed to the transformation of pristine structure to self-assembled stable structures during cycles, facilitating fast electron and ion diffusion. In solid-state electrolytes, the lattice distortion could change the site energies of alkali ions, promoting the generation of diffusion networks to enhance ionic conductivity. Despite such advancements, the development of HEBMs still faces substantial challenges. First, the compositional complexity of HEBMs complicates the understanding of reaction and stabilization mechanisms that require increasingly advanced structure-function studies. Second, many HEBMs contain expensive elements, increasing the cost. Third, there are significant difficulties in achieving compositional and size homogeneity of HEBM particles, necessitating research into sample preparation methods. Fourth, although possessing higher specific capacity than commercial LIB materials, HEBMs fall short of cycle performance targets. Therefore, more efforts in new materials exploration and understanding the mechanism of HE enhancement are urgently required to help realize the potential of HEBMs for comprehensive improvement in electrochemical performance and achieve practical application in high-performance LIBs/NIBs in the near future.

SUPPLEMENTAL INFORMATION

Supplemental information can be found online at <https://doi.org/10.1016/j.joule.2023.10.016>.

ACKNOWLEDGMENTS

W.Z. gratefully acknowledges the support of the China Scholarship Council (No. 202108430035). This work is supported by the Australian Research Council under grants DP200101862, DP210101486, and FL210100050.

AUTHOR CONTRIBUTIONS

W.Z. and G.L. proposed the topic of the perspective. W.Z., Q.L., and J.L. conducted the literature search. W.Z., G.L., and Q.L. wrote the manuscript. W.Z., Q.L., and J.A.Y. designed the figures. G.L., S.Z., V.K.P., and Z.G. discussed and revised the manuscript.

DECLARATION OF INTERESTS

The authors declare no competing interests.

REFERENCES

- Rost, C.M., Sachet, E., Borman, T., Moballegh, A., Dickey, E.C., Hou, D., Jones, J.L., Curtarolo, S., and Maria, J.P. (2015). Entropy-stabilized oxides. *Nat. Commun.* **6**, 8485.
- George, E.P., Raabe, D., and Ritchie, R.O. (2019). High-entropy alloys. *Nat. Rev. Mater.* **4**, 515–534.
- Oses, C., Toher, C., and Curtarolo, S. (2020). High-entropy ceramics. *Nat. Rev. Mater.* **5**, 295–309.
- Ma, Y., Ma, Y., Wang, Q., Schweidler, S., Botros, M., Fu, T., Hahn, H., Brezesinski, T., and Breitung, B. (2021). High-entropy energy materials: challenges and new opportunities. *Energy Environ. Sci.* **14**, 2883–2905.
- Liu, X., Li, X., Li, Y., Zhang, H., Jia, Q., Zhang, S., and Lei, W. (2022). High-entropy oxide: a future anode contender for lithium-ion battery. *EcoMat* **4**, e12261.
- Mao, J.F., Ye, C., Zhang, S.L., Xie, F.X., Zeng, R., Davey, K., Guo, Z.P., and Qiao, S.Z. (2022). Toward practical lithium-ion battery recycling: adding value, tackling circularity and recycling-oriented design. *Energy Environ. Sci.* **15**, 2732–2752.
- Bérardan, D., Franger, S., Meena, A.K., and Dragoe, N. (2016). Room temperature lithium superionic conductivity in high entropy oxides. *J. Mater. Chem. A* **4**, 9536–9541.
- Sarkar, A., Velasco, L., Wang, D., Wang, Q., Talasila, G., de Biasi, L., Kübel, C., Brezesinski, T., Bhattacharya, S.S., Hahn, H., et al. (2018). High entropy oxides for reversible energy storage. *Nat. Commun.* **9**, 3400.
- Wang, Q., Sarkar, A., Wang, D., Velasco, L., Azmi, R., Bhattacharya, S.S., Bergfeldt, T., Düvel, A., Heitjans, P., Brezesinski, T., et al. (2019). Multi-anionic and -cationic compounds: new high entropy materials for advanced Li-ion batteries. *Energy Environ. Sci.* **12**, 2433–2442.
- Zhao, C., Ding, F., Lu, Y., Chen, L., and Hu, Y.S. (2020). High-entropy layered oxide cathodes for sodium-ion batteries. *Angew. Chem. Int. Ed. Engl.* **59**, 264–269.
- Gu, Z.Y., Guo, J.Z., Cao, J.M., Wang, X.T., Zhao, X.X., Zheng, X.Y., Li, W.H., Sun, Z.H., Liang, H.J., and Wu, X.L. (2022). An advanced high-entropy fluorophosphate cathode for sodium-ion batteries with increased working voltage and energy density. *Adv. Mater.* **34**, e2110108.
- Fang, S., Bresser, D., and Passerini, S. (2020). Transition metal oxide anodes for electrochemical energy storage in lithium- and sodium-ion batteries. *Adv. Energy Mater.* **10**, 1902485.
- Jia, Y.G., Chen, S.J., Shao, X., Chen, J., Fang, D.-L., Li, S.S., Mao, A.Q., and Li, C.H. (2023). Synergetic effect of lattice distortion and oxygen vacancies on high-rate lithium-ion storage in high-entropy perovskite oxides. *J. Adv. Ceram.* **12**, 1214–1227.
- Ma, Y., Ma, Y., Dreyer, S.L., Wang, Q., Wang, K., Goonetilleke, D., Omar, A., Mikhailova, D., Hahn, H., Breitung, B., et al. (2021). High-entropy metal-organic frameworks for highly reversible sodium storage. *Adv. Mater.* **33**, e2101342.
- Stockham, M.P., Dong, B., and Slater, P.R. (2022). High entropy lithium garnets – testing the compositional flexibility of the lithium garnet system. *J. Solid State Chem.* **308**, 122944.
- Zeng, Y., Ouyang, B., Liu, J., Byeon, Y.W., Cai, Z.J., Miara, L.J., Wang, Y., and Ceder, G. (2022). High-entropy mechanism to boost ionic conductivity. *Science* **378**, 1320–1324.
- Zhang, R., Wang, C., Zou, P., Lin, R., Ma, L., Yin, L., Li, T., Xu, W., Jia, H., Li, Q., et al. (2022). Compositionally complex doping for zero-strain zero-cobalt layered cathodes. *Nature* **610**, 67–73.
- Yeh, J.-W., Chen, S.-K., Lin, S.-J., Gan, J.-Y., Chin, T.-S., Shun, T.-T., Tsau, C.-H., and Chang, S.-Y. (2004). Nanostructured high-entropy alloys with multiple principal elements: novel alloy design concepts and outcomes. *Adv. Eng. Mater.* **6**, 299–303.
- Wang, Q., Zhao, C., Wang, J., Yao, Z., Wang, S., Kumar, S.G.H., Ganapathy, S., Eustace, S., Bai, X., Li, B., et al. (2023). High entropy liquid electrolytes for lithium batteries. *Nat. Commun.* **14**, 440.
- Kim, S.C., Wang, J., Xu, R., Zhang, P., Chen, Y., Huang, Z., Yang, Y., Yu, Z., Oyakhire, S.T., Zhang, W., et al. (2023). High-entropy electrolytes for practical lithium metal batteries. *Nat. Energy* **8**, 814–826.
- Gao, M.C., Yeh, J.-W., Liaw, P.K., and Zhang, Y. (2016). *High-Entropy Alloys* (Springer International Publishing).
- Sarkar, A., Breitung, B., and Hahn, H. (2020). High entropy oxides: the role of entropy, enthalpy and synergy. *Scr. Mater.* **187**, 43–48.
- Tsai, M.-H., and Yeh, J.-W. (2014). High-entropy alloys: a critical review. *Mater. Res. Lett.* **2**, 107–123.
- Murty, B.S., Yeh, J.-W., Ranganathan, S., and Bhattacharjee, P. (2019). *High-Entropy Alloys* (Elsevier).
- Brahlek, M., Gazda, M., Keppens, V., Mazza, A.R., McCormack, S.J., Mielewczyk-Gryń, A., Musico, B., Page, K., Rost, C.M., Sinnott, S.B., et al. (2022). What is in a name: defining “high entropy” oxides. *APL Mater.* **10**, 110902.
- Delmas, C., Fouassier, C., and Hagenmuller, P. (1980). Structural classification and properties of the layered oxides. *Physica B+C* **99**, 81–85.
- Wang, K., Hua, W., Huang, X., Stenzel, D., Wang, J., Ding, Z., Cui, Y., Wang, Q., Ehrenberg, H., Breitung, B., et al. (2023).

- Synergy of cations in high entropy oxide lithium ion battery anode. *Nat. Commun.* **14**, 1487.
28. Li, W., Erickson, E.M., and Manthiram, A. (2020). High-nickel layered oxide cathodes for lithium-based automotive batteries. *Nat. Energy* **5**, 26–34.
 29. Li, J.X., Liang, G.M., Zheng, W., Zhang, S.L., Davey, K., Pang, W.K., and Guo, Z.P. (2022). Addressing cation mixing in layered structured cathodes for lithium-ion batteries: a critical review. Published online October 9, 2022. *Nano Mater. Sci.* <https://doi.org/10.1016/j.nanoms.2022.09.001>.
 30. Kim, J., Lee, H., Cha, H., Yoon, M., Park, M., and Cho, J. (2018). Prospect and reality of Ni-rich cathode for commercialization. *Adv. Energy Mater.* **8**, 1702028.
 31. Feng, X., Ren, D., He, X., and Ouyang, M. (2020). Mitigating thermal runaway of lithium-ion batteries. *Joule* **4**, 743–770.
 32. Fu, F., Liu, X., Fu, X., Chen, H., Huang, L., Fan, J., Le, J., Wang, Q., Yang, W., Ren, Y., et al. (2022). Entropy and crystal-facet modulation of P2-type layered cathodes for long-lasting sodium-based batteries. *Nat. Commun.* **13**, 2826.
 33. Huang, C.-Y., Huang, C.-W., Wu, M.-C., Patra, J., Xuyen Nguyen, T., Chang, M.-T., Clemens, O., Ting, J.-M., Li, J., Chang, J.-K., et al. (2021). Atomic-scale investigation of Lithiation/Delithiation mechanism in high-entropy spinel oxide with superior electrochemical performance. *Chem. Eng. J.* **420**, 129838.
 34. Hu, S.J., Pillai, A.S., Liang, G.M., Pang, W.K., Wang, H.Q., Li, Q.Y., and Guo, Z.P. (2019). Li-rich layered oxides and their practical challenges: recent progress and perspectives. *Electrochem. Energ. Rev.* **2**, 277–311.
 35. Zheng, W., Liang, G.M., Zhang, S.L., Davey, K., and Guo, Z.P. (2023). Understanding voltage hysteresis and decay during anionic redox reaction in layered transition metal oxide cathodes: a critical review. *Nano Res.* **16**, 3766–3780.
 36. Song, J., Ning, F., Zuo, Y., Li, A., Wang, H., Zhang, K., Yang, T., Yang, Y., Gao, C., Xiao, W., et al. (2023). Entropy stabilization strategy for enhancing the local structural adaptability of Li-rich cathode materials. *Adv. Mater.* **35**, e2208726.
 37. Liu, Y., Wang, D., Li, H., Li, P., Sun, Y., Liu, Y., Liu, Y., Zhong, B., Wu, Z., and Guo, X. (2022). Research progress in O3-type phase Fe/Mn/Cu-based layered cathode materials for sodium ion batteries. *J. Mater. Chem. A* **10**, 3869–3888.
 38. Kubota, K., and Komaba, S. (2015). Review—practical issues and future perspective for Na-ion batteries. *J. Electrochem. Soc.* **162**, A2538–A2550.
 39. Katcho, N.A., Carrasco, J., Saurel, D., Gonzalo, E., Han, M., Aguesse, F., and Rojo, T. (2017). Origins of bistability and na ion mobility difference in P2- and O3-Na_{2/3}Fe_{2/3}Mn_{1/3}O₂ cathode polymorphs. *Adv. Energy Mater.* **7**, 1601477.
 40. Yang, L., Chen, C., Xiong, S., Zheng, C., Liu, P., Ma, Y., Xu, W., Tang, Y., Ong, S.P., and Chen, H. (2021). Multiprincipal component P2-Na_{0.6}(Ti_{0.2}Mn_{0.2}Co_{0.2}Ni_{0.2}Ru_{0.2})O₂ as a high-rate cathode for sodium-ion batteries. *JACS Au* **1**, 98–107.
 41. Clément, R.J., Lun, Z., and Ceder, G. (2020). Cation-disordered rocksalt transition metal oxides and oxyfluorides for high energy lithium-ion cathodes. *Energy Environ. Sci.* **13**, 345–373.
 42. Wang, M., Chen, X., Yao, H., Lin, G., Lee, J., Chen, Y., and Chen, Q. (2022). Research progress in lithium-excess disordered rock-salt oxides cathode. *Energy & Environ. Materials* **5**, 1139–1154.
 43. Lun, Z., Ouyang, B., Kwon, D.H., Ha, Y., Foley, E.E., Huang, T.Y., Cai, Z., Kim, H., Balasubramanian, M., Sun, Y., et al. (2021). Cation-disordered rocksalt-type high-entropy cathodes for Li-ion batteries. *Nat. Mater.* **20**, 214–221.
 44. Goodenough, J.B., Hong, H.Y.-P., and Kafalas, J.A. (1976). Fast Na⁺-ion transport in skeleton structures. *Mater. Res. Bull.* **11**, 203–220.
 45. Jin, T., Li, H., Zhu, K., Wang, P.F., Liu, P., and Jiao, L. (2020). Polyanion-type cathode materials for sodium-ion batteries. *Chem. Soc. Rev.* **49**, 2342–2377.
 46. Li, H., Xu, M., Long, H., Zheng, J., Zhang, L., Li, S., Guan, C., Lai, Y., and Zhang, Z. (2022). Stabilization of multicationic redox chemistry in polyanionic cathode by increasing entropy. *Adv. Sci. (Weinh)* **9**, e2202082.
 47. Hurlbutt, K., Wheeler, S., Capone, I., and Pasta, M. (2018). Prussian blue analogs as battery materials. *Joule* **2**, 1950–1960.
 48. Patra, J., Nguyen, T.X., Tsai, C.C., Clemens, O., Li, J., Pal, P., Chan, W.K., Lee, C.H., Chen, H.T., Ting, J.M., et al. (2022). Effects of elemental modulation on phase purity and electrochemical properties of Co-free high-entropy spinel oxide anodes for lithium-ion batteries. *Adv. Funct. Mater.* **32**, 2110992.
 49. Zhao, Q., Stalin, S., Zhao, C.-Z., and Archer, L.A. (2020). Designing solid-state electrolytes for safe, energy-dense batteries. *Nat. Rev. Mater.* **5**, 229–252.
 50. Jung, S.K., Gwon, H., Kim, H., Yoon, G., Shin, D., Hong, J., Jung, C., and Kim, J.S. (2022). Unlocking the hidden chemical space in cubic-phase garnet solid electrolyte for efficient quasi-all-solid-state lithium batteries. *Nat. Commun.* **13**, 7638.
 51. Liu, Q., Zheng, W., Su, X., Zhang, X., Han, N., Wang, Z., Luo, J., Lu, Z., and Fransaer, J. (2023). Synergistic effect of different configurations on the anionic redox reaction in Na-deficient oxides for sodium ion batteries. *Chem. Eng. J.* **452**, 139337.
 52. Liu, Q., Zheng, W., Liu, G., Hu, J., Zhang, X., Han, N., Wang, Z., Luo, J., Fransaer, J., and Lu, Z. (2023). Realizing high-performance cathodes with cationic and anionic redox reactions in high-sodium-content P2-type oxides for sodium-ion batteries. *ACS Appl. Mater. Interfaces* **15**, 9324–9330.
 53. Sorkin, V., Yu, Z.G., Chen, S., Tan, T.L., Aitken, Z.H., and Zhang, Y.W. (2022). A first-principles-based high fidelity, high throughput approach for the design of high entropy alloys. *Sci. Rep.* **12**, 11894.
 54. Yao, Y., Liu, Z., Xie, P., Huang, Z., Li, T., Morris, D., Finckel, Z., Zhou, J., Jiao, M., Gao, J., et al. (2020). Computationally aided, entropy-driven synthesis of highly efficient and durable multi-elemental alloy catalysts. *Sci. Adv.* **6**, eaaz0510.
 55. Batchelor, T.A.A., Pedersen, J.K., Winther, S.H., Castelli, I.E., Jacobsen, K.W., and Rossmeisl, J. (2019). High-entropy alloys as a discovery platform for electrocatalysis. *Joule* **3**, 834–845.
 56. Ilya, T., Olivier, B., Sylvain, G., and Bernhard, S. (2018). Wasserstein auto-encoders. In *Proceedings of the 6th International Conference on Learning Representations (ICLR)*.
 57. Rao, Z., Tung, P.Y., Xie, R., Wei, Y., Zhang, H., Ferrari, A., Klaver, T.P.C., Körmann, F., Sukumar, P.T., Kwiatkowski da Silva, A., et al. (2022). Machine learning-enabled high-entropy alloy discovery. *Science* **378**, 78–85.
 58. Yao, L., Zou, P., Wang, C., Jiang, J., Ma, L., Tan, S., Beyer, K.A., Xu, F., Hu, E., and Xin, H.L. (2022). High-entropy and superstructure-stabilized layered oxide cathodes for sodium-ion batteries. *Adv. Energy Mater.* **12**, 2201989.
 59. Xiao, B.W., and Sun, X.L. (2018). Surface and subsurface reactions of lithium transition metal oxide cathode materials: an overview of the fundamental origins and remedying approaches. *Adv. Energy Mater.* **8**, 1802057.
 60. Yuan, K., Tu, T., Shen, C., Zhou, L., Liu, J., Li, J., Xie, K., and Zhang, G. (2022). Self-ball milling strategy to construct high-entropy oxide coated LiNi_{0.8}Co_{0.1}Mn_{0.1}O₂ with enhanced electrochemical performance. *J. Adv. Ceram.* **11**, 882–892.
 61. Chen, Y., Wang, T., Chen, H., Kan, W.H., Yin, W., Song, Z., Wang, C., Ma, J., Luo, W., and Huang, Y. (2023). Local structural features of medium-entropy garnet with ultra-long cycle life. *Matter* **6**, 1530–1541.
 62. Zuo, C., Hu, Z., Qi, R., Liu, J., Li, Z., Lu, J., Dong, C., Yang, K., Huang, W., Chen, C., et al. (2020). Double the capacity of manganese spinel for lithium-ion Storage by suppression of cooperative Jahn-Teller distortion. *Adv. Energy Mater.* **10**, 2000363.
 63. Yin, S., Deng, W., Chen, J., Gao, X., Zou, G., Hou, H., and Ji, X. (2021). Fundamental and solutions of microcrack in Ni-rich layered oxide cathode materials of lithium-ion batteries. *Nano Energy* **83**, 105854.
 64. Bi, Y.J., Tao, J.H., Wu, Y., Li, L., Xu, Y., Hu, E., Wu, B., Hu, J., Wang, C.M., Zhang, J.G., et al. (2020). Reversible planar gliding and microcracking in a single-crystalline Ni-rich cathode. *Science* **370**, 1313–1317.
 65. Seo, D.H., Lee, J., Urban, A., Malik, R., Kang, S., and Ceder, G. (2016). The structural and chemical origin of the oxygen redox activity in layered and cation-disordered Li-excess cathode materials. *Nat. Chem.* **8**, 692–697.
 66. Fan, Y.M., Olsson, E., Liang, G.M., Wang, Z.J., D'Angelo, A.M., Johannessen, B., Thomsen, L., Cowie, B., Li, J.X., Zhang, F.L., et al. (2023). Stabilizing cobalt-free Li-rich layered oxide cathodes through oxygen lattice regulation by

- two-phase Ru doping. *Angew. Chem. Int. Ed. Engl.* **62**, e202213806.
67. Lyu, Y., Wu, X., Wang, K., Feng, Z., Cheng, T., Liu, Y., Wang, M., Chen, R., Xu, L., Zhou, J., et al. (2021). An overview on the advances of LiCoO₂ cathodes for lithium-ion batteries. *Adv. Energy Mater.* **11**, 2000982.
68. Kalluri, S., Yoon, M., Jo, M., Park, S., Myeong, S., Kim, J., Dou, S.X., Guo, Z.P., and Cho, J. (2017). Surface engineering strategies of layered LiCoO₂ cathode material to realize high-energy and high-voltage Li-ion cells. *Adv. Energy Mater.* **7**, 1601507.
69. Liang, G., Wu, Z., Didier, C., Zhang, W., Cuan, J., Li, B., Ko, K.Y., Hung, P.Y., Lu, C.Z., Chen, Y., et al. (2020). A long cycle-life high-voltage spinel lithium-ion battery electrode achieved by site-selective doping. *Angew. Chem. Int. Ed. Engl.* **59**, 10594–10602.
70. Liang, G.M., Peterson, V.K., Wu, Z., Zhang, S., Hao, J., Lu, C.Z., Chuang, C.H., Lee, J.F., Liu, J., Leni c, G., et al. (2021). Crystallographic-site-specific structural engineering enables extraordinary electrochemical performance of high-voltage LiNi_{0.5}Mn_{1.5}O₄ spinel cathodes for lithium-ion batteries. *Adv. Mater.* **33**, 2101413.
71. Liang, G., Olsson, E., Zou, J., Wu, Z., Li, J., Lu, C.Z., D'Angelo, A.M., Johannessen, B., Thomsen, L., Cowie, B., et al. (2022). Introducing 4s-2p orbital hybridization to stabilize spinel oxide cathodes for lithium-ion batteries. *Angew. Chem. Int. Ed. Engl.* **61**, e202201969.
72. Zhang, S.D., Qi, M.Y., Guo, S.J., Sun, Y.G., Tan, X.X., Ma, P.Z., Li, J.Y., Yuan, R.Z., Cao, A.M., and Wan, L.J. (2022). Advancing to 4.6 V review and prospect in developing high-energy-density LiCoO₂ cathode for lithium-ion batteries. *Small Methods* **6**, e2200148.

Joule, Volume 7

Supplemental information

The promise of high-entropy materials

for high-performance rechargeable

Li-ion and Na-ion batteries

Wei Zheng, Gemeng Liang, Qiong Liu, Jingxi Li, Jodie A. Yuwono, Shilin Zhang, Vanessa K. Peterson, and Zaiping Guo

Supplemental information

Table S1. Crystal parameters for high entropy battery materials.

	Materials	Space group	<i>a</i> (Å)	<i>b</i> (Å)	<i>c</i> (Å)	<i>V</i> (Å ³)	α (°)	β (°)	γ (°)	Ref.
Cathodes	LiNi _{0.8} Mn _{0.13} Ti _{0.0} 2Mg _{0.02} Nb _{0.01} Mo 0.02O ₂	<i>R-3m</i>	2.8962	2.8962	14.28896	103.8	90	90	120	[1]
	Li _{1.0} [Li _{0.15} Mn _{0.50} Ni _{0.15} Co _{0.10} Fe _{0.0} 25Cu _{0.025} Al _{0.025} M g _{0.025}]O ₂	<i>C2/m</i>	4.94451(9)	8.57307(3)	5.0235(1)	/	90	109. 316	120	[2]
	Li _{1.3} Mn ²⁺ _{0.1} Co ²⁺ ₀ .1Mn ³⁺ _{0.1} Cr ³⁺ _{0.1} Ti 0.1Nb _{0.2} O _{1.7} F _{0.3}	<i>Fd-3m</i>	4.2544	4.2544	4.2544	77.0 04	90	90	90	[3]
	NaCu _{0.12} Ni _{0.12} M g _{0.12} Co _{0.15} Fe _{0.15} Mn _{0.1} Ti _{0.1} Sn _{0.1} S b _{0.04} O ₂	<i>R-3m</i>	3.02349(6)	3.02349(6)	16.0893(6)	124.9(2)	90	90	120	[4]
	Na _{0.6} (Ti _{0.2} Mn _{0.2} Co _{0.2} Ni _{0.2} Ru _{0.2}) O ₂	<i>P63/ mmc</i>	2.91455(1)	2.91455(1)	11.13772(9)	81.936 (1)	90	90	120	[5]
	Na _{3.4} Fe _{0.4} Mn _{0.4} V _{0.4} Cr _{0.4} Ti _{0.4} (PO 4) ₃	<i>R-3c</i>	8.7158	8.7158	21.7979	1434.05	90	90	120	[6]
	Na _x (FeMnNiCu Co)[Fe(CN) ₆]	<i>Fm- 3m</i>	10.271(1)	10.271(1)	10.271(1)	1083.4(4)	90	90	90	[7]
	Anodes	Mg _{0.2} Co _{0.2} Ni _{0.2} C u _{0.2} Zn _{0.2} O	<i>Fd-3m</i>	4.2330(6)	4.2330(6)	4.2330(6)	75.848	90	90	90
CrNiMnFeCu) ₃ O ₄		<i>Fd-3m</i>	8.346(2)	8.346(2)	8.346(2)	581.346	90	90	90	[9]
Gd(Co _{0.2} Cr _{0.2} F e _{0.2} Mn _{0.2} Ni _{0.2})O ₃		<i>Pbnm (62)</i>	5.220	5.466	7.589	216.53	90	90	90	[10]
Electrolyte	Li ₇ La ₃ Zr _{0.4} Hf _{0.4} S n _{0.4} Sc _{0.4} Ta _{0.4} O ₁₂	<i>Ia-3d</i>	12.94713	12.94713	12.94713	2170.238	90	90	90	[11]
	Li ₃ LaPrNdTeW O ₁₂	<i>Ia$\bar{3}d$</i>	12.58487(4)	12.58487(4)	12.58487(4)	1993.18(2)	90	90	90	[12]
	NaTi _{1/2} Zr _{1/2} Sn _{1/2} Hf _{1/2} P ₃ O ₁₂	<i>R-3c</i>	8.6607(2)	8.6607(2)	22.4023(5)	1455.24(7)	90	90	120	[12]
	LiTi _{1/2} Zr _{1/2} Sn _{1/2} Hf _{1/2} P ₃ O ₁₂	<i>R-3c</i>	8.6994(3)	8.6994(3)	21.6289(4)	1417.58(8)	90	90	120	[12]

Table S2. Summary for advantages and disadvantages of high entropy battery materials.

Structure	Material	Advantages	Disadvantages	Ref.	
Cathodes	Layered	<ul style="list-style-type: none"> ♦ Mitigate phase evolution during electrochemical process 	<ul style="list-style-type: none"> ♦ Increased fabrication cost due to the involvement of expensive elements 	[1]	
		<ul style="list-style-type: none"> ♦ Suppress oxygen loss and cation mixing 	<ul style="list-style-type: none"> ♦ Challenging to achieve particle homogeneity at the elemental level 	[2]	
		<ul style="list-style-type: none"> ♦ Suppress the low-potential redox couples Mn³⁺/Mn⁴⁺ 	<ul style="list-style-type: none"> ♦ Low initial coulombic efficiency of 85% 		
	Layered	<ul style="list-style-type: none"> ♦ Delay the phase evolution from O3 to P3 structure 	<ul style="list-style-type: none"> ♦ Low specific capacity of 110 mAh g⁻¹ ♦ Challenging to achieve particle homogeneity at the elemental level 	[4]	
		<ul style="list-style-type: none"> ♦ Mitigate Na⁺/vacancy ordering 	<ul style="list-style-type: none"> ♦ High cost due to the involvement of expensive Ru element 	[5]	
		<ul style="list-style-type: none"> ♦ Suppress phase evolution from P2 to OP4 phase 			
	Rock-salt	<ul style="list-style-type: none"> ♦ Create a percolating diffusion network to enhance rate performance 	<ul style="list-style-type: none"> ♦ Stabilize the crystal structure to restrain volume variation and phase transition 	<ul style="list-style-type: none"> ♦ Low air stability and easy to absorb water 	[13]
		<ul style="list-style-type: none"> ♦ Prevent the formation of a single dominant short-range order to preserve accessible O-TM percolation of Li transport 		<ul style="list-style-type: none"> ♦ Poor cycling performance (~60% after 20 cycles) 	[3]
		<ul style="list-style-type: none"> ♦ Introduce toxic element Cr 		<ul style="list-style-type: none"> ♦ Introduce toxic element Cr 	
	NASICON	<ul style="list-style-type: none"> ♦ Present a stable trigonal phase 	<ul style="list-style-type: none"> ♦ Challenging to achieve particle homogeneity at the elemental level 	[6]	
Prussian blue	<ul style="list-style-type: none"> ♦ Mitigate phase evolution 	<ul style="list-style-type: none"> ♦ Lower specific capacity of 100 mAh g⁻¹ 	[7]		

Anodes	Rock-salt	$Mg_{0.2}Co_{0.2}Ni_{0.2}Cu_{0.2}Zn_{0.2}O$	<ul style="list-style-type: none"> ◆ Improve structural stability 	<ul style="list-style-type: none"> ◆ High work voltage 	[8]
	Spinel	$(CrNiMnFeCu)_3O_4$	<ul style="list-style-type: none"> ◆ Enhance structural stability during cycles 	<ul style="list-style-type: none"> ◆ Introduce toxic element Cr ◆ High discharge voltage 	[9]
	Perovskite	$Gd(Co_{0.2}Cr_{0.2}Fe_{0.2}Mn_{0.2}Ni_{0.2})O_3$	<ul style="list-style-type: none"> ◆ Increase oxygen vacancies and mesoporous structure to enhance rate and cycling stability 	<ul style="list-style-type: none"> ◆ Introduce toxic element Cr ◆ High cost 	[10]
Electrolyte	Garnet	$Li_7La_3Zr_{0.4}Hf_{0.4}Sn_{0.4}Sc_{0.4}Ta_{0.4}O_{12}$	<ul style="list-style-type: none"> ◆ Decrease formation temperature ◆ Better reduction stability 	<ul style="list-style-type: none"> ◆ High cost ◆ Significant challenges in repetitive technique 	[11]
	NASICON/LISICON/garnet	Series of materials	<ul style="list-style-type: none"> ◆ Create a percolation network that enables enhanced ionic conductivity 	<ul style="list-style-type: none"> ◆ Increased fabrication cost due to the involvement of expensive elements ◆ Significant challenges in repetitive technique 	[12]
	Liquid electrolyte	Multiple salt in single dimethoxyethane solvent	<ul style="list-style-type: none"> ◆ Decrease the solvation strength ◆ Promote lithium ions diffusion ◆ Facilitate stable interphase passivation layers 	<ul style="list-style-type: none"> ◆ Increased fabrication cost due to the involvement of expensive elements 	[14]

Table S3. Comparison between high entropy battery materials and corresponding commercial battery materials.

	Material	Synthetic method	Specific capacity (mAh g ⁻¹)	Retention ^a	Thermal stability	Cost	Ref.
Cathodes	LiNi _{0.8} Mn _{0.13} Ti _{0.02} Mg _{0.02} Nb _{0.01} M _{0.02} O ₂	Co-precipitation and sintering	~205	1000	Better	Middle	[1]
	Li _{1.0} [Li _{0.15} Mn _{0.50} Ni _{0.15} Co _{0.10} Fe _{0.025} Cu _{0.025} Al _{0.025} Mg _{0.025}]O ₂	Sol-gel and sintering	~260	100	/	Middle	[2]
	LiCoO ₂	Solid-state sintering	135-150	500-1000	Low	High	[15]
	LiMn ₂ O ₄	Solid-state sintering	100-120	500-2000	Better	Low	[15]
	LiFePO ₄	Solid-state sintering	130-140	2000-6000	Great	Low	[15]
	LiNi _{1/3} Co _{1/3} Mn _{1/3} O ₂	Co-precipitation and sintering	155-220	800-2000	Low	Middle	[15]
Anodes	Mg _{0.2} Co _{0.2} Ni _{0.2} Cu _{0.2} Zn _{0.2} O	Solid-state and sintering	~650	500	/	Middle	[8]
	(CrNiMnFeCu) ₃ O ₄	Hydrothermal and sintering	~600	400	/	High	[9]
	Gd(Co _{0.2} Cr _{0.2} Fe _{0.2} Mn _{0.2} Ni _{0.2})O ₃	Sol-gel and sintering	~650	500	/	High	[10]
	Graphite	Multiple technique	300-370	>1000	Great	Low	[16]

^a The retention indicates the cycling numbers provided in the reference.

References

1. Zhang, R., Wang, C., Zou, P., Lin, R., Ma, L., Yin, L., Li, T., Xu, W., Jia, H., Li, Q., et al. (2022). Compositionally complex doping for zero-strain zero-cobalt layered cathodes. *Nature*, *610*, 67-73.
2. Song, J., Ning, F., Zuo, Y., Li, A., Wang, H., Zhang, K., Yang, T., Yang, Y., Gao, C., Xiao, W., et al. (2023). Entropy stabilization strategy for enhancing the local structural adaptability of Li-rich cathode materials. *Adv. Mater.*, *35*, e2208726.
3. Lun, Z., Ouyang, B., Kwon, D.H., Ha, Y., Foley, E.E., Huang, T.Y., Cai, Z., Kim, H., Balasubramanian, M., Sun, Y., et al. (2021). Cation-disordered rocksalt-type high-entropy cathodes for Li-ion batteries. *Nat. Mater.*, *20*, 214-221.
4. Zhao, C., Ding, F., Lu, Y., Chen, L. and Hu, Y.S. (2020). High-entropy layered oxide cathodes for sodium-ion batteries. *Angew. Chem. Int. Ed.*, *59*, 264-269.
5. Yang, L., Chen, C., Xiong, S., Zheng, C., Liu, P., Ma, Y., Xu, W., Tang, Y., Ong, S.P. and Chen, H. (2021). Multiprincipal component P2-Na_{0.6}(Ti_{0.2}Mn_{0.2}Co_{0.2}Ni_{0.2}Ru_{0.2})O₂ as a high-rate cathode for sodium-ion batteries. *JACS Au*, *1*, 98-107.
6. Li, H., Xu, M., Long, H., Zheng, J., Zhang, L., Li, S., Guan, C., Lai, Y. and Zhang, Z. (2022). Stabilization of multicationic redox chemistry in polyanionic cathode by increasing entropy. *Adv. Sci.*, *9*, e2202082.
7. Ma, Y., Ma, Y., Dreyer, S.L., Wang, Q., Wang, K., Goonetilleke, D., Omar, A., Mikhailova, D., Hahn, H., Breitung, B., et al. (2021). High-entropy metal-organic frameworks for highly reversible sodium storage. *Adv. Mater.*, *33*, e2101342.
8. Sarkar, A., Velasco, L., Wang, D., Wang, Q., Talasila, G., de Biasi, L., Kubel, C., Brezesinski, T., Bhattacharya, S.S., Hahn, H., et al. (2018). High entropy oxides for reversible energy storage. *Nat. Commun.*, *9*, 3400.
9. Patra, J., Nguyen, T.X., Tsai, C.C., Clemens, O., Li, J., Pal, P., Chan, W.K., Lee, C.H., Chen, H.Y.T., Ting, J.M., et al. (2022). Effects of elemental modulation on phase purity and electrochemical properties of Co-free high-entropy spinel oxide anodes for Lithium-ion batteries. *Adv. Funct. Mater.*, *32*, 2110992.
10. Jia, Y.G., Chen, S.J., Shao, X., Chen, J., Fang, D.-L., Li, S.S., Mao, A.Q. and Li, C.H. (2023). Synergetic effect of lattice distortion and oxygen vacancies on high-rate lithium-ion storage in high-entropy perovskite oxide. *J. Adv. Ceram.*, *12*, 1214-1227.
11. Wang, Q., Zhao, C., Wang, J., Yao, Z., Wang, S., Kumar, S.G.H., Ganapathy, S., Eustace, S., Bai, X., Li, B., et al. (2023). High entropy liquid electrolytes for lithium batteries. *Nat. Commun.*, *14*, 440.
12. Yan, Zeng, B.O., Yang, Jue, Liu, Young-Woon Byeon, Zijian Cai, Lincoln J. Miara, Yan Wang, Gerbrand Ceder. (2022). High-entropy mechanism to boost ionic conductivity. *Science*, *378*, 1320–1324.
13. Fu, F., Liu, X., Fu, X., Chen, H., Huang, L., Fan, J., Le, J., Wang, Q., Yang, W., Ren, Y., et al. (2022). Entropy and crystal-facet modulation of P2-type layered cathodes for long-lasting sodium-based batteries. *Nat. Commun.*, *13*, 2826.
14. Jung, S.K., Gwon, H., Kim, H., Yoon, G., Shin, D., Hong, J., Jung, C. and Kim, J.S. (2022). Unlocking the hidden chemical space in cubic-phase garnet solid electrolyte for efficient quasi-all-solid-state lithium batteries. *Nat. Commun.*, *13*, 7638.
15. Future Intelligence Unit. Lithium cathodes industry report: lithium manganese iron

phosphate and high nickel oxides are still the main direction.
<https://www.vzkoo.com/document/20220827961d426d3633c591dc42ecb6.html>.

16. SOHU. Lithium anodes industry report. [https:// www.sohu.com/a/607470099_121127986](https://www.sohu.com/a/607470099_121127986).